

Diffusion of Photoexcited Holes in a Viscous Electron Fluid


Yu. A. Pusep^{1,*}, M. D. Teodoro², V. Laurindo, Jr.², E. R. Cardozo de Oliveira², G. M. Gusev³, and A. K. Bakarov⁴

¹*São Carlos Institute of Physics, University of São Paulo, P.O. Box 369, 13560-970 São Carlos, São Paulo, Brazil*

²*Departamento de Física, Universidade Federal de São Carlos, 13565-905 São Carlos, São Paulo, Brazil*

³*Institute of Physics, University of São Paulo, 135960-170 São Paulo, São Paulo, Brazil*

⁴*Institute of Semiconductor Physics, 630090 Novosibirsk, Russia*

 (Received 30 May 2021; revised 3 February 2022; accepted 24 February 2022; published 30 March 2022)

The diffusion of photogenerated holes is studied in a high-mobility mesoscopic GaAs channel where electrons exhibit hydrodynamic properties. It is shown that the injection of holes into such an electron system leads to the formation of a hydrodynamic three-component mixture consisting of electrons and photogenerated heavy and light holes. The obtained results are analyzed within the framework of ambipolar diffusion, which reveals characteristics of a viscous flow. Both hole types exhibit similar hydrodynamic characteristics. In such a way the diffusion lengths, ambipolar diffusion coefficient, and the effective viscosity of the electron-hole system are determined.

DOI: [10.1103/PhysRevLett.128.136801](https://doi.org/10.1103/PhysRevLett.128.136801)

Specific characteristics of electron transport may strongly influence performance of microelectronic devices. In a dense electron system where the electron-electron collisions dominate over the collisions of electrons with disorder, the hydrodynamic approach is applied [1,2]. These conditions can be fulfilled in high mobility, correlated two-dimensional electron gas which leads to a variety of new phenomena associated with the hydrodynamic character of the electron gas, such as formation of density waves, shock waves, turbulence, solitons, etc. Many related specific effects were predicted and observed: the Gurzhi effect [3], choking of the electron fluid [4,5], Hagen-Poiseuille charge flow [6,7], hydrodynamic pumping effect [8], and Hall viscosity [9]. Particularly interesting is the system composed of electron and hole hydrodynamic components which interact through viscous friction. Hydrodynamic properties of such a system were considered in [10] where collective excitations and mutual electron-hole drag were studied. As for the drag effect, such effects caused by Coulomb interaction have been extensively demonstrated and investigated in a variety of systems including GaAs quantum well (QW) [11,12], double-QW electronic systems [13], and double-layer graphene [14]. However, to the best of our knowledge, so far no experiments have been performed in hydrodynamic electron-hole systems where drag effects are expected to be even stronger due to a viscous friction between the electron and hole components.

We address our investigation to the diffusion processes which take place in the hydrodynamic regime in a high-mobility mesoscopic GaAs channel. If the scattering on the channel edges is diffusive and the mean free path for electron-electron collisions, $l_{ee} \ll W$, where W is the channel width, the electron transport should take a form

of the hydrodynamic Poiseuille flow controlled by the electron shear viscosity $\nu \sim v_F l_{ee}$, where v_F is the Fermi velocity. In particular, we report on a photocurrent (PC) study of diffusion of the photogenerated holes within a viscous electron fluid. The question to be answered is whether optically injected holes will transform initially hydrodynamic electron system to a conventional Ohmic system, or a two-component electron-hole hydrodynamic system will arise.

A single 14 nm thick GaAs/AlGaAs QW was grown on (100)-oriented GaAs substrate by a molecular beam epitaxy. The sheet electron density and the mobility measured at the temperature of 1.4 K were $4.8 \times 10^{11} \text{ cm}^{-2}$ and $1.0 \times 10^6 \text{ cm}^2/\text{Vs}$, respectively. In this structure the viscous electron transport was demonstrated in Refs. [9,15,16].

Scanning PC microscopy experiments were performed on a multiterminal Hall bar structure with the 5 μm width and 100 μm length of the active at the temperature 3.7 K using a helium closed cycle cryostat equipped with a superconducting magnet (Attocube/Attodry1000). An electrically connected sample was placed on top of a x - y - z nanopositioner stack (Attocube), which allows for precise positioning of the laser beam focused by an aspheric objective ($NA = 0.64$) along the channel. The 532 nm illumination with the pump power about 0.5 mW from the laser (Cobolt/08) was focused onto the sample. The laser spot size is about 2 μm . The PC measurements were carried out by a source meter Keithley 2400. Time-resolved photoluminescence (PL) measurements were performed with the optical excitation achieved by a Pico Quant/LDH Series diode laser emitting 80 MHz pulses at 730 nm operated at an average pump power of 5 μW corresponding to a peak power of about 0.8 mW, which was chosen to generate the same number of electron-hole pairs

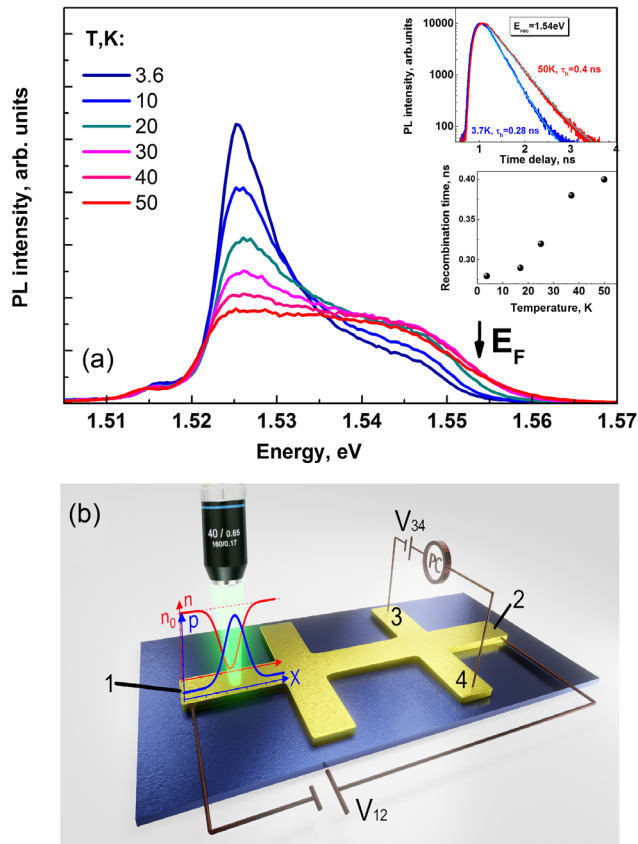


FIG. 1. (a) PL spectra of the GaAs/AlGaAs QW measured at various temperatures. Transients measured at the PL energy 1.54 eV at the point close to the collecting probes at $T = 3.7$ K (blue lines) and $T = 50$ K (red lines) are shown in the top inset, where the cyan lines are the best fits using a monoexponential decay function; the recombination times obtained by the best fits are shown in the bottom inset. (b) A sketch of the experimental configuration demonstrates electron n and hole p densities after photoexcitation as a function of the position along the channel and the electronic circuit that was attached to the sample; n_0 is the background electron concentration.

as in the case of the continuum laser. In this case emission was dispersed by a 75 cm Andor/Shamrock spectrometer and the PL transients were detected by a PicoQuant Hybrid PMT detector triggered triggered with a time correlated single photon PicoQuant/PicoHarp 300 counting system.

During the measurements the laser spot was scanned along the channel. The PC was measured using the potential probes of the Hall bar. Such configuration is usually employed to determine the diffusion length of the optically excited minority carriers: diffusion results in the PC value increasing with the decreasing distance between the probes and the laser spot. The solution of the one dimensional diffusion equation has a Gaussian shape with the exponent defined by the diffusion length. In such a case the diffusion length is obtained by fitting the calculated and measured PCs as a function of the distance.

The optical characterization of the QW structure studied here is shown in Fig. 1. The PL spectra depicted in Fig. 1(a) reproduce the joint density of states with the conduction band states populated below the Fermi level. The observed PL is determined by the recombination of the conduction band states below the Fermi level with holes in the valence band. In this case, the spectral width of the PL should be approximately equal to the Fermi energy. Indeed, the width of the PL spectra shown in Fig. 1(a) is in good agreement with the Fermi energy of 30 meV obtained in the same sample from magnetotransport measurements in [16]. The results of the PL time-resolved measurements shown in the panels (a),(b) reveal the recombination time increasing with temperature, what is expected in QWs with a degenerate electron system due to the phonon-assisted Auger recombination [17]. No significant variation of the recombination time along the channel is detected. The observed recombination time is attributed to the optical transitions between the conduction band and heavy hole valence band confined states.

A sketch of the experimental configuration is presented in Fig. 1(b). The electron and photogenerated hole densities after photoexcitation are shown as a function of the position along the mesoscopic channel. In the GaAs/AlGaAs heterostructure studied here, electron-hole pairs photogenerated in AlGaAs barriers are separated by a potential at the QW heterointerfaces: holes pass into the QW, while electrons nonradiatively recombine in the barriers. The recombination of holes injected in this way with background electrons reduces their concentration in the channel and, consequently, results in a minimum of the photocurrent measured between probes 3 and 4. Such a mechanism was found in Refs. [18–20].

The observed decrease in PC with a decrease in the distance between the laser spot and the collecting probes, shown in Fig. 2(a), manifests to a dominant role of recombination between holes and electrons injected into the channel. Such a process is expected in high-mobility QWs where the recombination time τ is shorter than the electron transport relaxation time. Thus, the system under study consists of the background electrons and the photo-generated holes, in which diffusion proceeds in an ambipolar form.

The Hall bar sample studied here shown in Fig. 2(b) has eight potential probes. All the potential probes revealed identical PC responses. The PC measured as a function of the laser spot position along the channel using the probes 3,4 and 5,6 are depicted in Fig. 2(a). In the following, the data obtained with the collecting probes 3,4 are demonstrated.

Worth mentioning that the current measured between the potential probes shown in Fig. 2(a) consists of the current due to the voltage applied to the probes and the photocurrent itself. However, throughout the article we will call this current photocurrent, because it directly demonstrates the effect of electron-hole recombination.

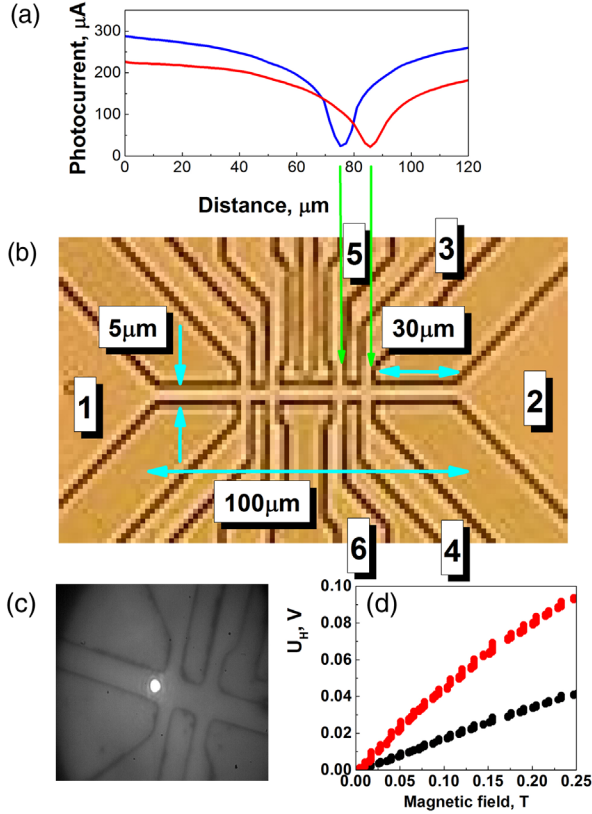


FIG. 2. (a) Photocurrent measured at $T = 3.7$ K with collecting probes 34 (red line) and 56 (blue line), (b) microscope image of the sample with the characteristic dimensions, (c) the sample image with the laser spot focused to the channel, and (d) Hall voltages U_H measured on collecting probes 3 and 4, at a current $I_{12} = 0.13$ mA between the probes 1 and 2, in the dark (black circles) and at an average laser pump power of $5 \mu\text{W}$ (red circles).

To prove the reduction in the number of electrons observed under laser illumination, we measured the Hall voltage across the collecting contacts without and with laser excitation, when the laser was focused on the channel area between the contacts. The obtained data shown in Fig. 2(d) indeed confirm a twofold decrease in the electron concentration under illumination.

The results shown in Figs. 2(a) and 2(d) imply the concentration of holes injected to the QW, comparable to the electron background concentration. In such a case the diffusion takes a form of an ambipolar electron-hole diffusion.

As stated above, the specific scattering conditions establish the viscous electron flow in the sample studied here. At the same time it is unclear whether such conditions apply to photogenerated holes. In order to define a character of the photogenerated hole diffusion the diffusion profiles were measured at different temperatures.

In the hydrodynamic approach the electron-electron, hole-hole, and electron-hole scattering dominates over

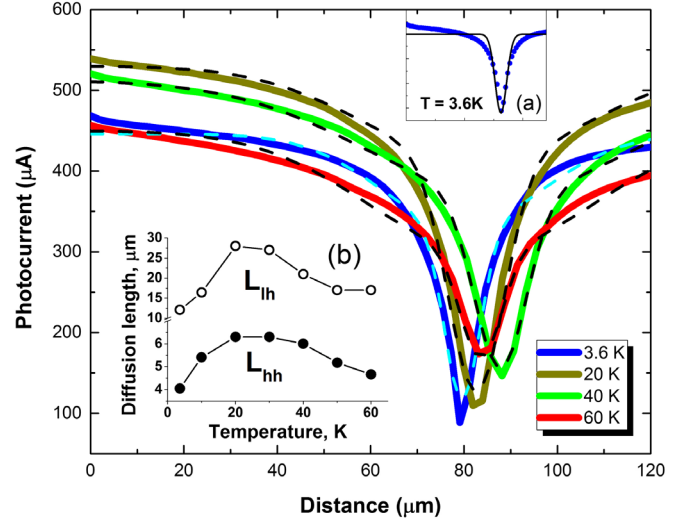


FIG. 3. Photocurrent measured at different temperatures at $U_{34} = 2$ V as a function of the distance along the channel (solid lines). The dashed lines were calculated according to Eq. (1) with the contributions of both heavy and light holes. The panel (a) shows the fit of the photocurrent measured at $T = 3.6$ K by Eq. (1) with the contribution of only heavy holes. The panel (b) shows the diffusion lengths of heavy and light holes as a function of the temperature.

the scattering of electrons and holes with disorder. In such a case diffusion reveals characteristics of viscous flow: the diffusion length should increase with the increasing temperature. In the case considered here, an increase in the diffusion length of the photogenerated holes with temperature will show that they exhibit hydrodynamic properties.

The PC measured at different temperatures shown in Fig. 3 is determined by the doping electron concentration, which decreases due to recombination with holes when they arrive the collecting contacts. The net electron concentration that contributes to the PC can be expressed as $n(x) = n_0 - n_h(x)$, where n_0 is the doping background electron concentration in the absence of photoexcitation and $n_h(x)$ is the concentration of photogenerated holes, which is represented by the Gaussian profile. As shown in Fig. 3(a), the PC calculated in this way as a function of the distance between the laser spot and the collecting contacts does not fit the experimental diffusion profile. A considerable deviation is found at long distances, which is a signature of an additional diffusion flow. A possible cause of this additional flow can be presence of light holes generated by the light.

Following the approach presented above, the net electron concentration can be calculated according to the formula

$$n(x) = n_0 - n_{hh} \exp\left(-\frac{x^2}{4L_{hh}^2}\right) - n_{lh} \exp\left(-\frac{x^2}{4L_{lh}^2}\right), \quad (1)$$

where the second and third terms are associated with the heavy and light holes arriving at the collecting probes, $n_{hh(lh)}$ is the heavy hole (light hole) concentrations, while L_{hh} and L_{lh} are the diffusion lengths of the heavy and light holes, respectively. Then the PC as a function of distance can be calculated as $j_{PC}(x) = en(x)v_F$. A good accordance between the experimental data and the PC calculated by Eq. (1) manifests to the simultaneous diffusion of the heavy and light holes. The diffusion lengths obtained by the best fits are shown in the panel (b) as a function of temperature. The shorter diffusion length is associated with the heavy hole flow, while the longer one is due to the light holes. Up to 30 K both diffusion lengths increase with increasing temperature, while higher temperatures result in decreasing of the diffusion lengths. The diffusion length increasing with temperature manifests itself in a viscous flow. For temperatures higher than about 35 K, strong polar LO-phonon scattering determines the momentum relaxation time in GaAs QWs. In this case phonon scattering dominates over the electron-electron collisions and diffusion takes a common form.

Thus, the presented results demonstrate formation of the electron-hole plasma composed by the electrons and injected holes in the studied here mesoscopic GaAs channel. At low temperatures diffusion of this plasma reveals viscous character.

The PC measured as a function of the distance with different voltages U_{34} applied to the probes 3 and 4 is shown in Fig. 4(a). The best fits of the experimental PC diffusion profiles using Eq. (1) are shown in Fig. 4(a). The obtained diffusion lengths L_{hh} and L_{lh} are found slightly decreasing with the increasing U_{34} voltages.

In the following, the effect of the electron-hole drag is investigated using an external electric field applied parallel to the diffusion flow. The application of the longitudinal voltage U_{12} makes it possible to control the number of photogenerated carriers arriving at the collecting probes. Diffusion profiles obtained with different U_{12} values when negative and positive potentials are applied to contacts 1 and 2, respectively, and with fixed $U_{34} = 1$ V are shown in Fig. 4(b). In this case an apparent asymmetry of the diffusion profile is found. Such a change of the diffusion profile reveals a drift of electrons in the external electric field which drag photogenerated holes. From the left side of the collecting probes, the flow of electrons carries holes to the collecting contacts, facilitating their diffusion. In this case, holes located farther from the collecting probes contribute to PC. While on the right side, electrons carry holes away from the contacts. Accordingly, drift of the injected photo holes against the electric field is observed due to their entrainment by the drift electron current.

It should be noted that the drift of the minority electrons against the electric field caused by negative absolute mobility was observed in p -doped GaAs QWs in [11,12]. Moreover, it was argued that this should result

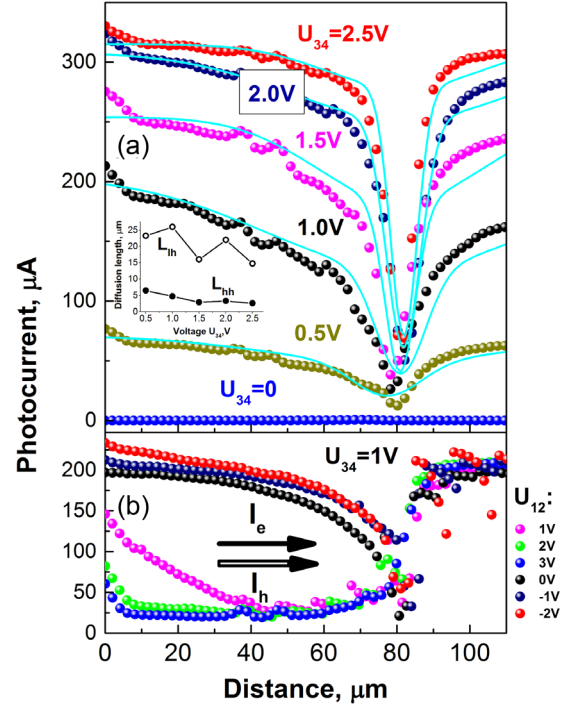


FIG. 4. Photocurrent measured at $T = 3.7$ K as a function of distance along the channel with different U_{34} (a) and U_{12} (b) voltages. The solid lines in the panel (a) are calculated according to Eq. (1), while the diffusion length of heavy and light holes are depicted in the inset. The directions of the electron drift I_e and the hole flow I_h along the channel are shown corresponding to the positive U_{12} voltage.

in the negative photoconductivity. Such an effect indeed may reduce the photoconductivity in the case when the momentum relaxation time is much shorter than the electron-hole recombination time. However, in the samples studied here the high electron mobility implies the momentum relaxation time longer than or equal to the recombination time. In these conditions the recombination process dominates over the transport which suggests the recombination as a principal reason for the observed decrease in PC. In addition, according to [12], the negative photoconductivity is not expected at high excitation, when the density of photogenerated carriers approaches the density of the majority carriers.

It is interesting to note that in this case the PC diffusion profile reveals asymmetric shape. This performance of the observed electron-hole drag is very different from that found in the diffusion electron-hole system [11,12], where Gaussian-like diffusion profiles were observed. The observed asymmetry of the diffusion shape implies a very strong drag effect, which is likely caused by additional viscous friction between electrons and holes.

It is worth noting that the observed drag effect can explain the diffusion length decreasing with the increasing voltage applied to the collecting probes, shown in the inset to Fig. 4(a). Namely, the current flowing through the

collecting contacts entrain the holes arriving the contacts resulting in easier diffusion.

With the purpose to describe the observed diffusion the following analysis is performed. The diffusion length of the viscous particles can be calculated following the formalism presented in Ref. [21]. The fluid viscosity leads to shear flow along the x direction with a velocity $v_x(y)$ which varies in the y direction. The diffusion transfers momentum. In a one-dimensional shear flow the momentum density only has an x component:

$$M_x = \rho v_x(y), \quad (2)$$

where ρ is the fluid density. In the considered case the momentum flux is given by the expression

$$T_{xy} = D \left(\frac{\partial M_x}{\partial y} \right) = \rho D \left(\frac{\partial v_x}{\partial y} \right), \quad (3)$$

where D is the diffusion coefficient. On the other hand, by a definition a viscous flux $T_{xy} = \eta(\partial v_x/\partial y)$ with the dynamic viscosity coefficient η . As a result, $\eta = \rho D$. The kinematic (shear) viscosity of a fluid is defined as $\nu \equiv \eta/\rho$. Thus, in the case of a one-dimensional diffusion the kinematic viscosity ν and the diffusion coefficient of the involved particles are the same quantity [22]. Finally, the diffusion length of the viscous fluid is $L_D = \sqrt{D\tau}$ where τ is the particle lifetime (in the case studied here it is the recombination time).

In the case of the ambipolar diffusion studied here the diffusion length is attributed to the mutual diffusion of electrons and holes. Using the diffusion length $L_{hh} = 5 \mu\text{m}$, together with the heavy hole recombination time $\tau = 2.8 \times 10^{-10}$ s yield the ambipolar diffusion coefficient and consequently, the effective viscosity coefficient $D_a = \nu_a = 0.09 \text{ m}^2/\text{s}$. The obtained effective viscosity coefficient is found 3 times smaller than that of electrons $\nu_e \approx 0.3 \text{ m}^2/\text{s}$, determined in the same structure by nonlocal electrical measurements [16].

In summary, the diffusion of photogenerated holes was studied by means of a scanning PC microscopy carried out on a mesoscopic channel formed in a high-mobility GaAs QW where the electrons reveal hydrodynamic properties. As a result, the diffusion of the photogenerated holes was investigated within the viscous fluid of the electrons. It was shown that the hole system consists of heavy and light holes. Diffusion lengths of both hole types were obtained. Depending on the temperature, two diffusion regimes were observed: hydrodynamic regime at temperatures below 30 K and common diffusion at higher temperatures. Both types of holes exhibited similar hydrodynamic properties. The drift of photogenerated holes against external electric field was found due to the hole drag by viscous electrons. In this case the corresponding diffusion profiles

were found very different from those in the usual diffusion electron-hole system. The obtained results were analyzed within the framework of ambipolar diffusion. In such a way the ambipolar diffusion coefficient and the effective viscosity of the electron-hole system were determined. The presented results differ from the hydrodynamic effects observed so far in viscous electron systems, since in the reported case the diffusion of holes occurs within a mixture consisting of the hydrodynamic electrons and the injected photo holes. Thus, the obtained results manifest to the formation of a three-component hydrodynamic system formed by background electrons and injected heavy and light holes.

Financial support from the Brazilian agencies FAPESP (Grant No. 2015/16191-5), CNPq (Grant No. 305837/2015-0), CAPES (Grant No. PNPd 88887.336083/2019-00) are gratefully acknowledged.

*pusep@ifsc.usp.br

- [1] A. V. Andreev, S. A. Kivelson, and B. Spivak, *Phys. Rev. Lett.* **106**, 256804 (2011).
- [2] D. A. Bandurin, I. Torre, R. Krishna Kumar, M. Ben Shalom, A. Tomadin, A. Principi, G. H. Auton, E. Khestanova, K. S. Novoselov, I. V. Grigorieva, L. A. Ponomarenko, A. K. Geim, and M. Polini, *Science* **351**, 1055 (2016).
- [3] R. N. Gurzhi, *Sov. Phys. JETP* **17**, 521 (1963).
- [4] M. I. Dyakonov and M. S. Shur, *Phys. Rev. Lett.* **71**, 2465 (1993).
- [5] M. I. Dyakonov and M. S. Shur, *Phys. Rev. B* **51**, 14341 (1995).
- [6] L. W. Molenkamp and M. J. M. de Jong, *Phys. Rev. B* **49**, 5038 (1994).
- [7] M. J. M. de Jong and L. W. Molenkamp, *Phys. Rev. B* **51**, 13389 (1995).
- [8] A. O. Govorov and J. J. Heremans, *Phys. Rev. Lett.* **92**, 026803 (2004).
- [9] G. M. Gusev, A. D. Levin, E. V. Levinson, and A. K. Bakarov, *Phys. Rev. B* **98**, 161303(R) (2018).
- [10] D. Svintsov, V. Vyurkov, S. Yurchenko, T. Otsuji, and V. Ryzhii, *J. Appl. Phys.* **111**, 083715 (2012).
- [11] R. A. Höpfel, J. Shah, P. A. Wolff, and A. C. Gossard, *Phys. Rev. Lett.* **56**, 2736 (1986).
- [12] R. A. Höpfel, J. Shah, P. A. Wolff, and A. C. Gossard, *Phys. Rev. B* **37**, 6941 (1988).
- [13] J. P. Eisenstein and A. H. MacDonald, *Nature (London)* **432**, 691 (2004).
- [14] R. V. Gorbachev, A. K. Geim, M. I. Katsnelson, K. S. Novoselov, T. Tudorovskiy, I. V. Grigorieva, A. H. MacDonald, S. V. Morozov, K. Watanabe, T. Taniguchi, and L. A. Ponomarenko, *Nat. Phys.* **8**, 896 (2012).
- [15] G. M. Gusev, A. D. Levin, E. V. Levinson, and A. K. Bakarov, *AIP Adv.* **8**, 025318 (2018).
- [16] A. D. Levin, G. M. Gusev, E. V. Levinson, Z. D. Kvon, and A. K. Bakarov, *Phys. Rev. B* **97**, 245308 (2018).
- [17] A. S. Polkovnikov and G. G. Zegrya, *Phys. Rev. B* **58**, 4039 (1998).
- [18] A. S. Chaves, A. F. S. Penna, J. M. Worlock, G. Weimann, and W. Schlapp, *Surf. Sci.* **170**, 618 (1986).

- [19] D. Richards, G. Fasol, and K. Ploog, *Appl. Phys. Lett.* **57**, 1099 (1990).
- [20] M. Hayne, A. Usher, A. S. Plaut, and K. Ploog, *Phys. Rev. B* **50**, 17208 (1994).
- [21] A. Achterberg, *Gas Dynamics. An Introduction with Examples from Astrophysics and Geophysics* (Atlantis Press, 2016), ISBN 978-94-6239-194-9.
- [22] A. Achterberg (unpublished).